N 87-26020

NUMERICAL SIMULATION OF UNSTEADY VISCOUS FLOWS

Wilbur L. Hankey
Wright State University

Abstract

Most unsteady viscous flows may be grouped into two categories, i.e., forced and self-sustained oscillations. Examples of forced oscillations occur in turbomachinery and in internal combustion engines while self-sustained oscillations prevail in vortex shedding, inlet buzz and wing flutter. Numerical simulation of these phenomena have been achieved due to the advancement of the vector processor computer. Recent progress in the simulation of unsteady viscous flows is addressed in this paper.

1.0 Introduction

Unsteady flows have always been an important subject of fluid mechanics. Rotating turbomachinery, turbulence, flutter, buzz, buffet, aircraft spin, autorotation, noise and vortex shedding are common examples. Although these topics were subjected to intensive analysis in the past, the fluid mechanics community had to rely on experiment to produce the necessary design information. Fortunately, CFD now offers the potential for providing future design details based upon first principle computations.

Early CFD efforts concentrated on producing steady solutions, even though time-dependent methods were used, but only as an iteration technique. The introduction of the vector processor computer with higher computational speed has now made unsteady calculations possible. This paper will present a survey of some of the recent progress made in the field of unsteady viscous flows. Most unsteady flows may be divided into two categories, i.e., forced oscillations and self-sustained oscillations. In a forced oscillation an external force adds work to the fluid. Computationally this means an unsteady boundary condition must be prescribed. In a self-sustained oscillation no external forcing function is imposed, therefore, the boundary conditions are steady. According to Den Hartog (1947) the distinguishing difference between these two categories is that the force will still exist in a forced oscillation if one stops the motion, while in a self-sustained oscillation stopping the motion will also remove the force.

Before embarking on a numerical investigation, it is well to perform a linear analysis of an unsteady flow in order to gain insight into the fundamental physics (Hankey, 1980).

2.0 Linearized Analysis of Unsteady Fluid Flows

Consider a two-dimensional parallel flow of an incompressible, inviscid (but rotational) fluid. The governing equations are as follows:

$$\nabla \cdot \underline{V} = 0 \tag{2.1}$$

$$\rho \frac{D\underline{V}}{Dt} = -\nabla p \tag{2.2}$$

The mean flow is assumed to be parallel and rotational with small perturbations of the following form assumed:

$$\begin{aligned} u &= \bar{u}(y) + u'(x,y,t) \\ v &= \quad\; v'(x,y,t) \\ p &= p_\infty + p'(x,y,t) \end{aligned} \tag{2.3}$$

Inserting these relationships into the governing equations and retaining only first order terms produces a linear system of equations.

$$u'_x + v'_y = 0 \tag{2.4}$$

$$\zeta'_t + \bar{u}\zeta'_x = \bar{u}_{yy} v' \tag{2.5}$$

where

$$\zeta' = v'_x - u'_y = \text{vorticity} \tag{2.6}$$

Disturbances of the following form are assumed

$$v' = \phi(y)\, e^{i\alpha(x-ct)} \tag{2.7}$$

$$\text{where} \quad c = c_r + i\, c_i \tag{2.8}$$

c_r = propagation velocity
c_i = amplification factor
α = wave number

Substitution of this relationship into the governing equation produces the Rayleigh equation (Rayleigh, 1880) which is a degenerate Orr-Sommerfeld equation appropriate for large Reynolds numbers)

$$\phi'' - \left(\alpha^2 + \frac{\bar{u}''}{\bar{u}-c}\right)\phi = 0 \tag{2.9}$$

with boundary conditions requiring that disturbances vanish at the wall and at the undisturbed outer edge.

$$\phi(0) = 0 \qquad \text{and} \qquad \phi(\infty) = 0$$

For prescribed values of $\bar{u}$ this is an eigenvalue problem in which $c(\alpha)$ can be obtained subject to the boundary condition constraint. The resulting solution takes on the following form:

$$v' = \phi e^{\alpha c_i t}\, e^{i\alpha(x-c_r t)} \tag{2.10}$$

For positive values of c_i an instability occurs which is equivalent to a negative damping case. Rayleigh (1880) first investigated this type of flow and proved that velocity profiles with inflection points are unstable. In order to further explore this fact, a class of separated flows was analyzed. The stability of Stewartson's Lower Branch solutions of the Falkner-Skan equation was investigated. The Rayleigh equation was solved for several different values of the pressure gradient parameter, β, for the entire range of separated flows from incipient to a free shear layer (Verma, et al. 1979). Figure 2. represents the values of the amplification factor for the unstable frequency range. (Note $f = \alpha_r c_r/2\pi\sigma$). For reference purposes, these amplification factors are nearly two orders of magnitude greater than the more familiar Tollmien-Schlichting waves. The propagation speed (c_r) for the disturbances was generally between 0.4 and 0.9 of u_e. Therefore, one can deduce from these results that flow instabilities do exist (positive c_i) but over a very limited frequency range for similar separated laminar boundary layers. By analogy, the frequency for which maximum c_i occurs can be viewed as the natural frequency of the shear layer. This corresponds to the most probable Strouhal number likely to occur for periodic disturbances and is always numerically less than unity. In Reference 5, compressibility effects of a free shear layer were investigated and the instability was found to diminish as Mach number increased (Figure 2.2). Although only one class of flows with inflection points has been examined, one is tempted to generalize these findings for all separated flows. One can speculate that (Den Hartog, 1947) separated flows become more unstable in progressing from incipient to fully separated; (Hankey, 1980) separated flows possess a relatively low natural frequency for which they are most likely to be self-excited and are stable on either side of that frequency; (Rayleigh, 1880) the instability diminishes as Mach number increases. Based upon these hypotheses, one can embark upon an analysis of unsteady flow problems.

3.0 Linear Oscillator Model

Separated flows were shown to possess a natural frequency for which small disturbances are highly amplified over a limited frequency range. However, for a self-sustained oscillation to persist a continuous string of disturbances is required to excite the shear layer. In this section the mechanism necessary to attain this result will be discussed.

It is informative at this point to compare a fluid dynamic oscillator with an electronic oscillator (Glassford, 1965). To create an electronic oscillator the circuit must contain an amplifier with a positive feedback loop (Figure 3.1). A self-excited fluid dynamic oscillator therefore must also contain these two components. In the previous section the shear layer was shown to play the role of the amplifier. The feedback loop is postulated to be a subsonic path in which pressure waves (acoustical signals) are returned to the shear layer origin and selectively reamplified.

The condition for oscillator resonance can be ascertained by examining the transfer functions for the two components.

If A in Figure 3.1 is the transfer function (a complex number) of the amplifier and B is the transfer function of the feedback loop, then the overall gain is as follows:

$$\text{Gain} = \frac{A}{1-AB} \tag{3.1}$$

The existence of a frequency for which the return ratio, AB, equals unity is a sufficient condition for infinite gain and is hence the criterion for a sustained oscillation.

To summarize, three ingredients are necessary to produce an oscillator, i.e., (Den Hartog, 1947) amplifier with, (Hankey, 1980) positive feedback at (Rayleigh, 1880) a return ratio of unity.

Examination of the linear equations for a self-excited oscillation identifies the essential components and predicts the resonant frequency. However, it provides no capability to predict the amplitude of the disturbance or produce detailed flow field features for large disturbances. To proceed further it becomes necessary to examine the nonlinear characteristics, i.e., Navier-Stokes equations. This will be accomplished in the next section.

4.0 PROCEDURE FOR NUMERICALLY SOLVING THE NAVIER-STOKES EQUATIONS

4.1 Governing Equations

The two-dimensional or axisymmetric Navier-Stokes equations for a compressible perfect gas are listed below (7,8). This system of equations will be used to analyze several cases involving self-excited oscillations discussed later in this paper.

$$U_t + E_x + y^{-k}(y^k F)_y = k\, y^{-k} H \tag{4.1}$$

where

$$U = \begin{matrix}\rho\\ \rho u\\ \rho v\\ \rho e\end{matrix}; \qquad E = \begin{matrix}\rho u\\ \rho u^2-\sigma_{11}\\ \rho uv-\tau\\ \rho ue-u\sigma_{11}-v\tau-kT_x\end{matrix}$$

$$F = \begin{matrix}\rho v\\ \rho uv-\tau\\ \rho v^2-\sigma_{22}\\ \rho ve-v\sigma_{22}-u\tau-kT_y\end{matrix}; \qquad H = \begin{matrix}0\\ 0\\ -\sigma_{\phi\phi}\\ 0\end{matrix} \tag{4.2}$$

and

$$\tau=\mu(u_y+v_x) \qquad \sigma_{11}=-p-2/3\mu\nabla\cdot\underline{V}+2\mu u_x$$

$$e=C_vT+\frac{u^2+v^2}{2} \qquad \sigma_{22}=-p-2/3\mu\nabla\cdot\underline{V}+2\mu v_y$$

$$p=\rho RT \qquad \sigma_{\phi\phi}=-p-2/3\mu\nabla\cdot\underline{V}+2\mu\frac{v}{y}$$

$$\nabla\cdot\underline{V}=u_x+y^{-k}(y^k v)_y$$

k = 0 for 2 dimensional flow
k = 1 for axisymmetric flow

This system of equations contains four dependent variables (u,v,T,p) where μ, k, C_v and R are prescribed for the gas. The three independent variables (x,y,t) are expressed in a Cartesian framework. A Cartesian system is unsatisfactory for most problems and therefore a general coordinate transformation must be employed. The physical space (x,y) is mapped into computational domain (ξ,η) where numerical calculations are performed.

4.2 Boundary Conditions

Four types of boundary conditions are required for the cases to be computed, i.e., (a) wall, (b) inflow, (c) outflow, and (d) symmetry surfaces. These shall now be addressed.

(a) Wall (η=0)

On an impermeable wall a no-slip condition for the velocity is required.

$$u(\eta=0)=0$$
$$v(\eta=0)=0$$

The wall temperature is also specified.

$$T(\eta=0)=Tw$$

The pressure on the wall does not require a boundary condition but must be determined from the flow field equations. The finite difference algorithm does require specification of a pressure relation at the wall and therefore a "compatibility condition" is used which is obtained from a degenerate normal momentum equation, i.e.,

$$\frac{\partial p}{\partial n}(\eta=0) = 0 \cong 0 \quad \text{to order } Re^{-1}$$

(b) Inflow (ξ=0)

At the inflow surface all flow variables are prescribed using characteristic variables.

U = constant for self-sustained oscillations
U = U(t) = temporally specified for forced oscillations

$$U = \begin{matrix} p/\rho^{\gamma} \\ v \\ u+p/\rho_\infty a_\infty \\ u-p/\rho_\infty a_\infty \end{matrix}$$

Note: One notable exception is that for subsonic flows the gradient of the last characteristic variable is set to zero.

(c) Outflow (ζ=L)

At a downstream boundary in which outflow occurs a simple wave equation is used to minimize reflections.

$$U_t + c_r U_s = 0$$

where s is aligned with the main streamline.

$$U = \begin{matrix} p/\rho^{\gamma} \\ v \\ u+p/\rho_\infty a_\infty \\ u-p/\rho_\infty a_\infty \end{matrix}$$

c_r = propagation velocity of disturbances.

$$c_r = \begin{matrix} u_\infty \\ u_\infty \\ u_\infty + a_\infty \\ u_\infty - a_\infty \end{matrix}$$

(d) Symmetry (y=0)

For axisymmetric flows the axis requires a symmetry condition as follows:

$$v(y=0) = 0$$
$$u_y(y=0) = 0$$
$$T_y(y=0) = 0$$
$$p_y(y=0) = 0$$

This concludes the description of the principle boundary conditions for the problems to be investigated. These four types are not implied to be a complete set to be used to investigate all flows but are representative of the type used in many present day calculations. Research is in progress in this area to improve the description of boundary conditions; especially for subsonic flows.

5.0 NUMERICAL RESULTS OF SELF-SUSTAINED OSCILLATIONS

In the previous section the numerical procedure was described for solving the time-dependent Navier-Stokes equations. In this section the results of several large scale computations will be explored. The configurations investigated include a cylinder, spike tipped body, inlet, cone, and dump combustor configuration.

5.1 CYLINDER

The periodic shedding of large scale eddies from a cylinder immersed in a flowing stream is probably the most commonly recognized self-sustained oscillation in fluid mechanics. A stability analyses of a series of potential vortices representing this flow was accomplished by Von Karman (1911). This wake analysis of the "Karman Vortex Street" unfortunately contains little information about the true physics of the phenomenon and hence further investigation is required. Von Karman was limited at that time since the only tool available was linear potential theory. Today, however, the computer provides us with the ability to numerically integrate the Navier-Stokes equations and investigate problems of this type.

In Reference 10, the flow behind a cylinder at a Mach number of 0.6 and a Reynolds number of 1.7×10^5 was computed and compared with an experiment for similar conditions (Owen, 1981). By use of the techniques described in Section 4, the time dependent flow over a cylinder was determined by numerically integrating the Navier-Stokes equations. No turbulence model was used

for this case since the cylinder was in the subcritical (laminar) regime at this Reynolds number. Therefore, all large scale "turbulent" eddies in the wake were computed based upon first principles.

The flow was impulsively started. All points in the field were initially at the free stream state and suddenly the nonslip boundary condition on the cylinder walls applied. Initially, symmetric vortices developed behind the cylinder which became asymmetric after one cycle period and developed into periodic asymmetric vortex shedding after about three periods. The wall pressure history for the 90° and 270° polar angle location covering over twenty cycles of oscillation is shown in Figure 5.1.

The computed Strouhal number, fd/u, was 0.21; in general agreement with experiment. Numerically computed Reynolds stresses for the wake are presented in Figure 5.2 The comparison is favorable considering only large scale, low frequency eddies were simulated. This investigation shows that it is possible to numerically generate the production of large scale turbulent eddies and generally duplicate the experiment without accurately simulating the dissipation of the fine scale structure.

The mean-velocity wake profile possesses two inflection points. A linear stability analysis of this profile (Betchov, 1967) shows two unstable modes to exist due to these two inflection points. The first mode produces an asymmetric oscillation while the second mode (with a lower amplification factor) produces a symmetric one. Since the asymmetric mode has the greater amplification, this accounts for the observed asymmetric serpentine wake pattern behind the cylinder. The Strouhal number, f d/u, for which the amplification factor is maximum is 0.2. The symmetric mode still exists, however, although lower in amplitude and higher in frequency. This tends to explain the modulation by a higher frequency of the wave form (Figure 5.1).

5.2 Buzz of Spikes

The numerical solutions of the time dependent Navier-Stokes equations for the cylinder confirmed the linear oscillation model for a self-oscillation, i.e., (a) the shear layer with an inflection point is the fluid dynamic amplifier; (b) feedback is achieved by acoustic waves returning to the origin; (c) resonance occurs at discrete integer values of the fundamental frequency when the return signal is "in phase" with the original disturbance. The existence of all three features is required to produce a self-excited oscillation. The removal of any one feature should eliminate the oscillation. (In most practical flight problems, the oscillation is undesirable and must be avoided.) The elimination characteristics of the oscillation shall now be discussed.

A configuration to demonstrate this phenomenon is a blunt body with a spike tip operating a supersonic speed. Spike tipped bodies are noted for producing violent buzz under a restricted range of spike lengths (Harney, 1979). Figure 5.3 shows the experimental pressure intensity for different spike lengths at a Mach number of three. Buzz exists, but only for spike lengths above 20 mm for this configuration. Oscillations are not encountered at shorter lengths. Separated flow will always occur in the concave region between the spike and face of the blunt-nose body, and hence, amplification is always present. However, resonance will not occur if the spike length is less than one wavelength of the unstable wave (α critical). Two numerical calculations were conducted (Shang et al., 1980) for spike lengths of 13 mm and 39 mm. The shorter spike length had an $\frac{L}{\delta}$ of 1.5 and resulted in a stable flow. However, the longer spike length (39 mm) had an $\frac{L}{\delta} = 9$ and produced a self excited oscillation comparable to the experiment. The spike pressure history comparison is shown in Figure 5.4. The spectral analysis for both computation and experiment is depicted in Figure 5.5. Outstanding agreement is observed between the computation and experiment for frequency, amplitude and wave form, showing the ability of the numerics to simulate self-excited oscillations.

5.3 Inlet Buzz

A supersonic inlet operating at subcritical flow conditions possesses the necessary features for buzz, i.e., a large region of intermittent separated flow and a downstream interface to reflect acoustical signals. When an inlet with a supersonic diffuser is throttled back to subcritical flow conditions, the normal shock is expelled from the diffuser causing separation on the centerbody. This separated shear layer is unstable and the principal cause of the oscillation. Standing waves occur in the duct. The upstream end of the inlet behaves as an open end (pressure node) while the downstream end behaves as a closed end (pressure antinode). Antisymmetric modes occur with all harmonics being odd. Two very significant results can be obtained from this standing wave analysis. First, the frequencies should be commensurable in which harmonics occur at exact integer values of the fundamental frequency. Secondly, antisymmetric mode shapes occur in the duct. One can also anticipate frequency modes to jump discretely to the next integer eigenvalue as flow conditions are changed by different throttle settings. This indeed is the experimental finding (Hankey, 1980).

One calculation (Newsome, 1983) using the complete Navier-Stokes equations for inlet buzz has been accomplished and compared with experimental data (Nagashim, 1972). An external compression axisymmetric inlet and diffuser configuration was modeled for flow conditions corresponding to a Mach two free stream with a Reynolds number based upon 6 cm diameter of $Re_D = 2.36 \times 10^6$. Because the turbulence model was found to artificially damp the occurrence of instabilities it was deleted from the program. The justification for the omission is that the numerical code is capable of resolving a finite number of low frequency components up to the shortest wave length ($2\Delta x$). Current turbulence models over-predict the appropriate eddy viscosity. When the turbulence model is omitted,

the turbulent transport process is resolvable while the turbulent dissipative processes is not. This approach was used to compute through three buzz cycles. The instability developed immediately as a consequence of the non-equilibrium state of the initial conditions. A sequence of Mach contours covering the third buzz cycle is shown in Figure 5.6. During buzz the bow shock was forced to the tip of the centerbody as a result of the interaction with a reflected compression wave. In the expulsion phase a region of reverse flow extended between the base of the bow shock and the cowl lip. As the shock reached the centerbody tip, the shear layer ruptured and flow was spilled. The bow shock remained in this position for a time corresponding to the propagation and reflection of an expansion wave from the downstream choked throat. The inlet then ingested mass and the shock retreated to the cowl lip with the flow reattaching to the centerbody.

5.4 Boundary Layer Transition

As alluded to in previous sections, a portion of the turbulence spectrum can be resolved in computing self-excited oscillations. One then wonders if boundary layer transition can be simulated numerically as a self-excited oscillation on todays' computers. To explore this area, the onset of transition was computed for a hypersonic boundary layer (Hankey, 1982). For highly compressible flow, the generalized inflection point, $(\rho u')'=0$, replaces the low speed Rayleigh condition of $u''=0$. At hypersonic speed, linear theory shows that the second mode instability dominates (which is fortunately two dimensional). Examination of this case by use of the linear stability theory results of Mack (1965) showed the numerical computation to be feasible. Numerical solution of the time dependent Navier Stokes equations was accomplished (with steady boundary conditions) using step sizes sufficiently small to resolve the unstable waves predicted from linear theory. The configuration was a 7° cone at a Mach number of 8 and a Reynolds number of 10^6 based on a one meter length. Temperature fluctuations with a regular periodic behavior were obtained in the numerical computation. The amplitude of these self-excited waves varied across the boundary layer with a maximum occurring near the edge. Good agreement was obtained with experiment for both the temperature and velocity fluctuations (Figure 5.7).

A comparison of the computed spectral analysis (Figure 5.8) with experiment shows agreement in the frequency at peak amplitude, however, the experiment has a broader band. Further, research is required to resolve the disparity, however, the results are encouraging for the first phase in the prediction of turbulence.

5.5 Dump Combustor

The flow in an efficient combustor must be inherently unsteady in order to enhance mixing and expell the burned products before they quench the flame. A computation of cold flow in a dump combustor was accomplished in order to ascertain if the vortex shedding phenomenon could be simulated (Guelda, 1987). Figure 5.9 is a time sequence of vortex patterns computed for a dump combustor configuration with choked flow at the nozzle exit. The sequence shows periodic shedding and downstream propagation of the vortices. Also, shown in Figure 5.10 is a comparison of the computed pressure histograms with the experimental (Davis, 1981) for three different locations. These results show encouragement in the ability to numerically simulate unsteady viscous flows.

6.0 Forced Oscillations

Forced oscillations in unsteady viscous flows occur in examples, such as the piston motion of an internal combustion engine, movement of an aircraft control surface, rotation of a turbine blade in a jet engine, flapping of a bird's wing, and pumping of blood through the heart. In all cases, an external force adds work to the fluid to produce a desired result. To simulate these forced oscillations, the time-dependent Navier Stokes equations must be used. Time dependent boundary conditions and 3-D adaptive grid systems are required. This field is certainly a challenge for the CFD community of the future. In the interim more modest, yet still challenging efforts, are in progress.

6.1 Turbomachine Rotor-Stator Stage

Rai (1985) simulated the motion of a 2-D rotor-stator stage of a turbomachine and produced an impressive movie of the flow field. Scott (1985) also simulated a similar case by imposing a stator time-varying wake profile onto a multiple-blade rotor and obtained the temporal flow features. The case computed depicted the combination of 54 stator and 72 rotor blades of a compressor stage. Figure 6.1 displays the flow field for four rotor blades at one instant in time.

6.2 Acoustically Excited Jet

Another form of forced oscillation is the acoustic excitation of a shear layer. Since a shear layer possesses a "natural frequency," a resonance type phenomenon occurs when the shear layer is exited near this frequency. Acoustic excitation regularizes the quasi-periodic vortex shedding of the self-sustained oscillations in a shear layer. This modest excitation results in higher amplitudes and enhanced mixing of the jet. Figure 6.2 is a comparison between the experimental (Scott, 1985) and computed vortex patterns (Scott, 1986) of a jet for an excitation Strouhal number of 0.45.

6.3 Dynamic Lift

Still another type of forced oscillation is the rapid rotation of a wing (such as a helicopter blade) to produce dynamic lift. The sudden change in angle of attack creates a starting vortex which migrates through the flow field. During this transient phase, the dynamic lift coefficient exceeds the static lift value but later falls below before recovering to the static value. This phenomenon is also of interest for

the dynamic maneuvering of an aircraft in the post-stall regime.

Figure 6.3 is an example of a numerical calculation (Tassa, 1981) of the dynamic lift coefficient for an airfoil under high rotational pitch rate.

7.0 Summary

Self-excited and forced oscillations in fluid flows have been analyzed. The concept of a fluid amplifier within a separated shear layer was presented. Signals entering the shear layer are selectively amplified over a limited frequency range and returned through a feedback loop as acoustic pressure waves. Resonance occurs when the return signal is "in phase" with the original disturbance wave. Under these circumstances no external forcing function is required and a self-excited oscillation can occur. If a forced excitation signal is imposed on a shear layer at its "natural frequency," resonance occurs. Linear theory is useful in predicting the frequency of the instability and providing a qualitative description of the phenomenon. Quantitative description of unsteady viscous flows are possible through the numerical solution of the time dependent Navier-Stokes equations.

REFERENCES

ATWJA, K.K.; and LEPICOVSKY, J.: Acoustic Control of Free Jet Mixing. AIAA 85-0569, Free Shear Flow Control Conference, Boulder, CO, Mar. 1985.

BETCHOV, R.; and CRIMINALE, W.: Stability of Parallel Flows, New York Academic Press, p 37-40, 1967.

DAVIS, D.L.: Coaxial Dump Ramjet Combustor Combustion Instabilities. AFWAL TR-81 2047, July, 1981.

DEN HARTOG, J.P.: Mechanical Vibrations. McGraw-Hill Book Co., Inc. 1947.

GIELDA, T.; SCOTT, J.N.; and HANKEY, W.L.: Investigation of Unsteady Flow in a Dump Combustor Configuration (to be published).

GLASFORD, G.M.: Linear Analysis of Electronic Circuits, Addison-Wesley, 1965.

HANKEY, W.: Analysis of Inlet Buzz. AFWAL-TM-FIMM-1980.

HANKEY, W.L.; and SHANG, J.S.: Analysis of Self-Excited Oscillations in Fluid Flows. AIAA-80-1346, Snowmass, CO, 14-16 July, 1980.

HANKEY, W.L.; and SHANG, J.S.: Natural Transition - A Self-Excited Oscillation. AIAA Paper No. 82-1011, AIAA/ASME Conference, St. Louis, MO, June, 1982.

HARNEY, D.J.: Oscillating Shocks on Spiked Nose Tips at Mach 3. AFFDL-TM-79 9-FX, 1979.

MACCORMACK, R.W.: Numerical Solutions of the Interactions of a Shock Wave with Laminar Boundary Layer. Lecture notes in physics, Vol. 59, Springer Verlag, 1976.

MACK, L.M.: The Stability of the Compressible Laminar Boundary Layer According to a Direct Numerical Solution. AGARDograph 87, Pt. 1, pp 329-362, May 1965.

NAGASHIM, T.; OBKATT, T.; and ASANUMA, T.: Experiment of Supersonic Air Intake Buzz. Report No. 481. University of Tokyo, 1972.

NEWSOME, R.W.: Numerical Simulation of Near-Critical and Unsteady Subcritical Inlet Flow Fields. AIAA Paper No. 83-0175, Jan 1983.

OWEN, F.K.; and JOHNSON, D.A.: Measurements of Unsteady Vortex Flow Field. AIAA Journal, Vol. 18, pp 1173-1179.

RAI, M.M.: Navier-Stokes Simulations of Rotor-Stator Interaction Using Patched and Overlaid Grids. AIAA Paper No. 85-1519, Jul. 1985.

RAYLEIGH, LORD: On the Stability or Instability of Certain Fluid Motion. Scientific Papers, Vol. 1, pp. 474-484, Cambridge University Press, 1880.

ROSCOE, D.; and HANKEY, W.L.: Stability of Compressible Shear Layers. AFWAL-TR-80-3016, April 1980.

SCOTT, J.N.: Numerical Simulation of Unsteady Flow in a Compressor Rotor Cascade. AIAA 85-0133, 23rd Aerospace Sciences Meeting, Reno, NV, Jan. 1985.

SCOTT, J.N.; and HANKEY, W.L.: Numerical Simulation of Unsteady Flow in an Axisymmetric Shear Layer. AIAA 86 0202, 24th Aerospace Sciences Meeting, Reno, NV, Jan. 1986.

SHANG, J.; SMITH, R.; and HANKEY, W.: Flow Oscillations of Spike Tipped Bodies. AIAA Paper 80-0062.

SHANG, J.S.; BUNING, P.G.; HANKEY, W.L.; and WIRTH, M.C.: Performance of a Vectorized Three Dimensional Navier-Stokes Code on the CRAY-1 Computer. AIAA J., Vol. 18, No. 9, pp. 1073-1079, Sept 1980.

SHANG, J.S.: Oscillatory Compressible Flow Around a Cylinder. AIAA Paper No. 82-0098, 1982.

TASSA, Y; and SANKAR, J.L.: Dynamic Stall of an Oscillating Airfoil in Turbulent Flow Using Time Dependent Navier-Stokes Solver. IUTAM Symposium on Unsteady Turbulent Shear Flows, Toulouse, France, 1981.

VERMA, G.; HANKEY, W.L.; and SCHERR, S.: Stability Analysis of the Lower Branch Solutions of the Falkner-Skan Equations. AFFDL-TR-79-3116, July 1979.

VON KARMAN, T.; and Nachr. d. wiss. ges. gottinger: Mathe. Phys. Klasse, 509 (1911).

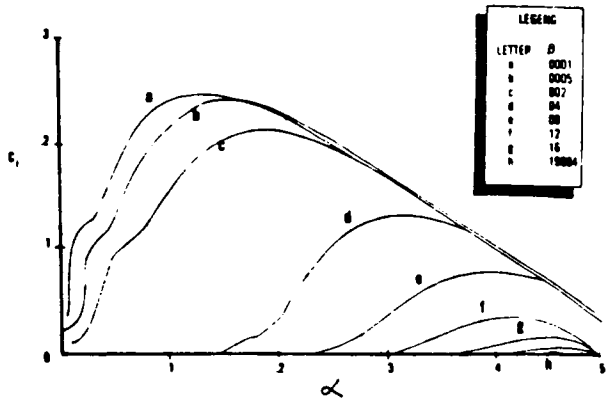

2.1 Amplification Factor vs. Wave Number for Various β (Ref 4)

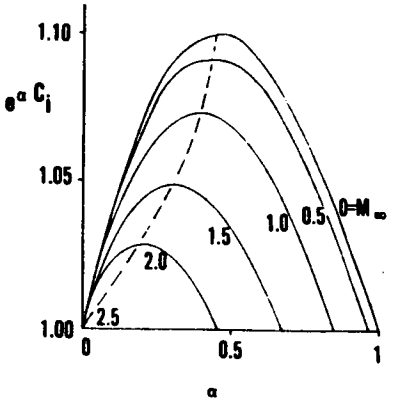

2.2 Variation of C_i with α for Various Mach Number

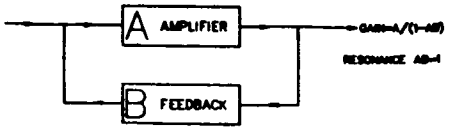

3.1 Diagram of Oscillator with Feedback

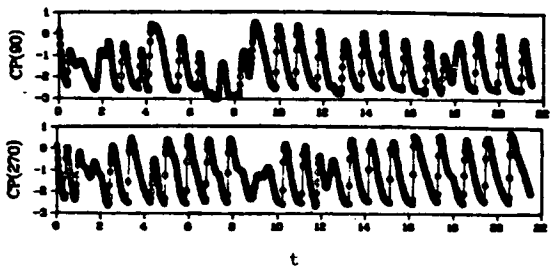

5.1 Temporal Evolution of Pressure Coefficient

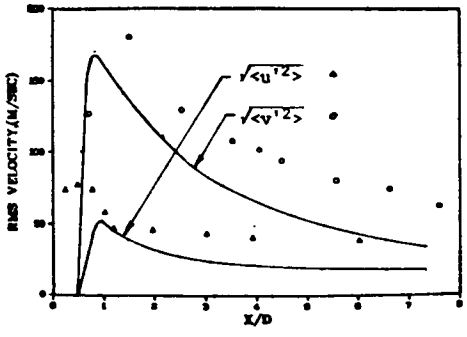

5.2 Comparison of Turbulent Intensity (Data Ref F.K. Owen and D.A. Johnson, 1981)

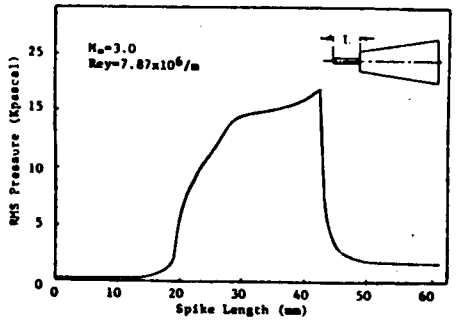

5.3 RMS Pressure Level for Spike Buzz

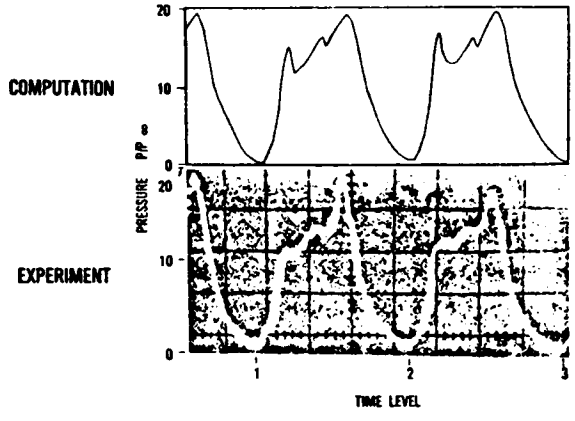

5.4 Comparison of Predicted and Experimental Wave Forms for Spike-Buzz

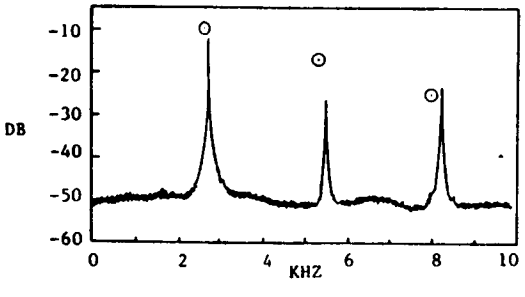

5.5 Comparison of Predicted and Experimental Spectral Analysis for Spike-Buzz

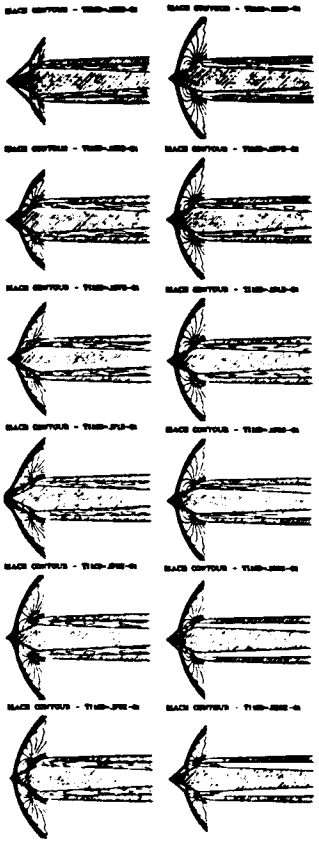

5.6 Forebody Flow Field, Third Buzz Cycle

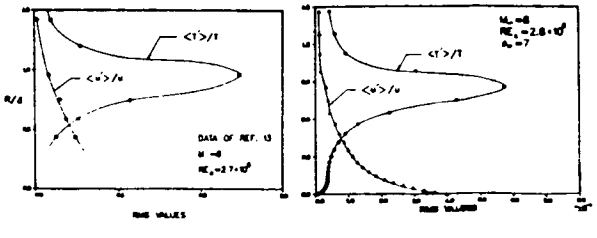

5.7 Computed RMS Profiles of Temperature and Velocity

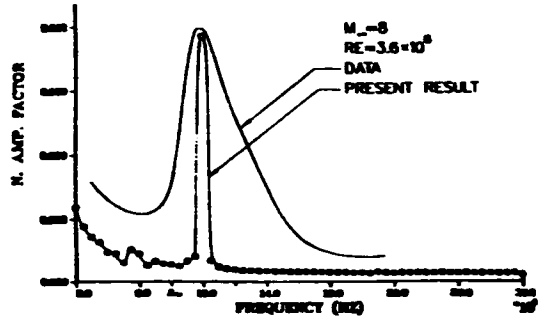

5.8 Spectral Analysis for Instability over Cone

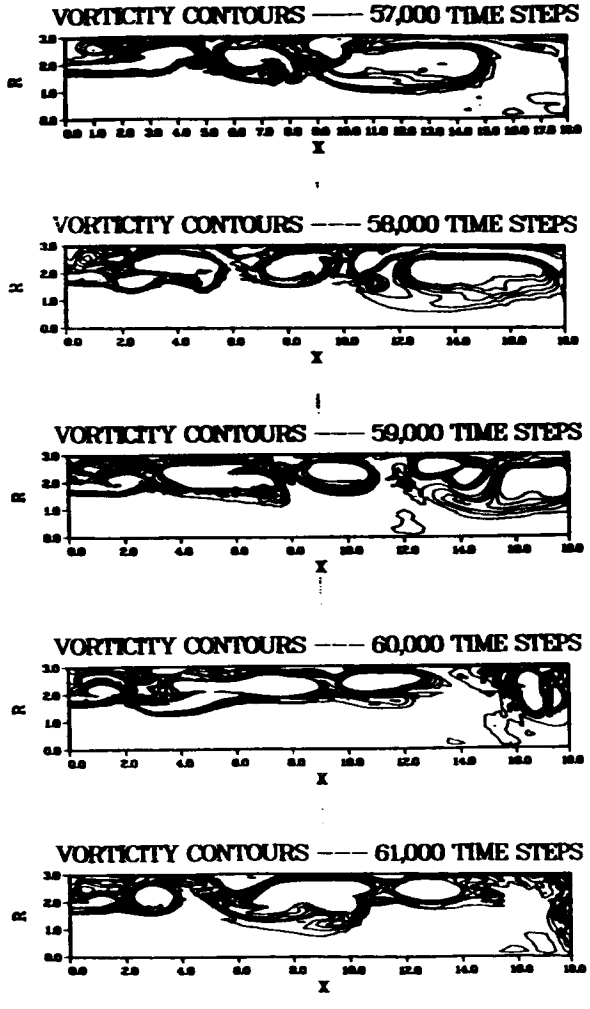

5.9 Vortex Sequence for Dump Combustor

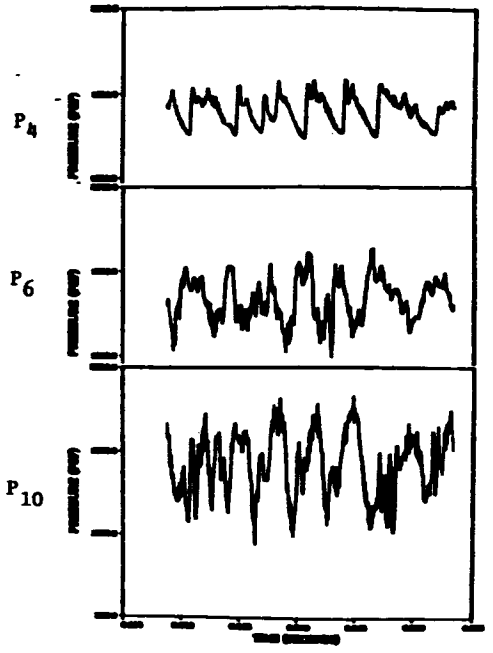

Theory

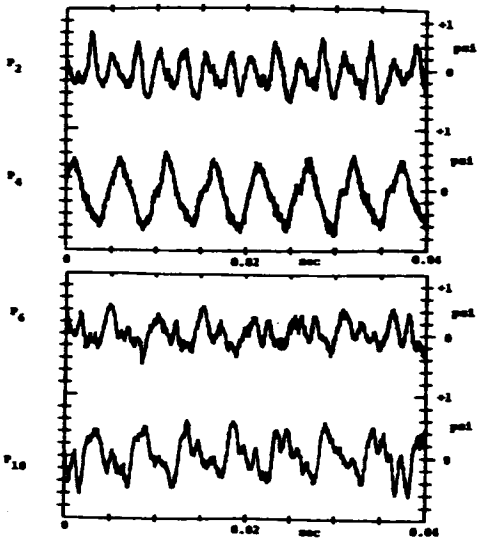

Experiment

5.10 Pressure Histogram Comparison

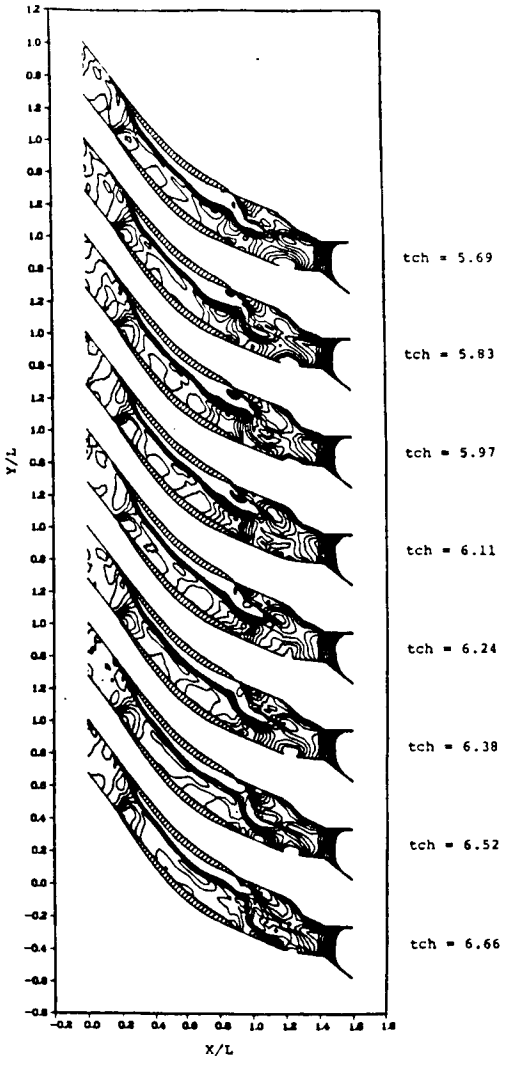

6.1 Compressor Cascade Flow Field History

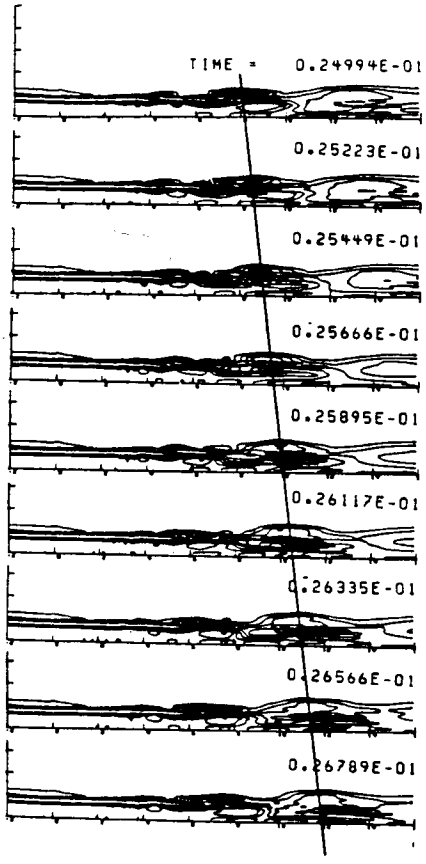

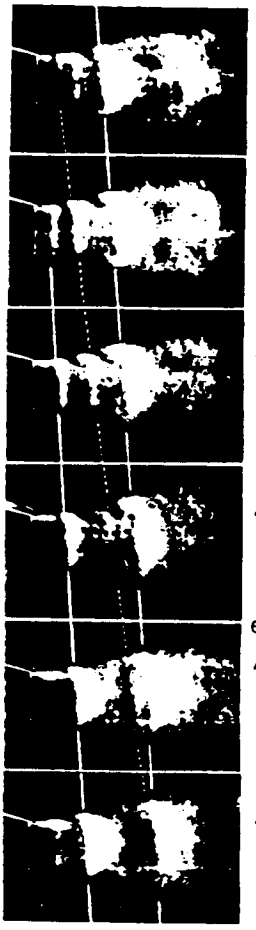

M_j = 0.29, T_t = 673 K,
St_j = 0.25, L_e = 144 dB

6.2 Comparison of Vortex Structure for Excited Jet Theory/Experiment

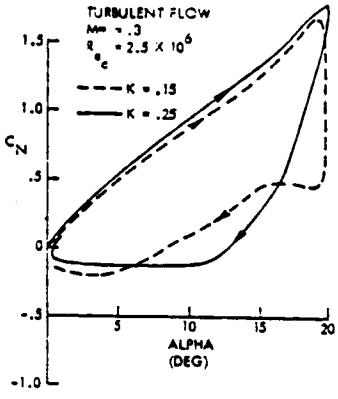

6.3 Dynamic Lift Hysterisis